TECHNICAL NOTE

Visualization of Hemodynamics in a Silicon Aneurysm Model Using Time-Resolved, 3D, Phase-Contrast MRI

H. Isoda
M. Hirano
H. Takeda
T. Kosugi
M.T. Alley
M. Markl
N.J. Pelc
H. Sakahara

SUMMARY: We performed time-resolved 3D phase-contrast MR imaging by using a 1.5T MR scanner to visualize hemodynamics in a silicon vascular model with a middle cerebral aneurysm. We ran an aqueous solution of glycerol as a flowing fluid with a pulsatile pump. Time-resolved images of 3D streamlines and 2D velocity vector fields clearly demonstrated that the aneurysm had 3D complex vortex flows within it during systolic phase. This technique provided us with time-resolved 3D hemodynamic information about the intracranial aneurysm.

Flow dynamics in intracranial aneurysms and their adjacent parent vessels are believed to play an important role in the development and rupture of intracranial aneurysms.[1] The ideal method for visualizing intracranial hemodynamics would be in vivo blood flow analysis in which we can quickly and inexpensively acquire accurate blood flow information from each patient. Phase contrast MR imaging might be a promising noninvasive method for analyzing in vivo intracranial aneurysmal hemodynamics for living human beings in the future. Tateshima et al[2] reported that the phase contrast MR imaging method was able to depict the complex 3D intraaneurysmal flow in an acrylic aneurysm model, although 3D visualization of hemodynamics seemed to be insufficient because of the limitation of the number of imaging sections.

Time-resolved 3D phase-contrast MR imaging (4D-Flow) to obtain human hemodynamics in 4 dimensions was developed recently and with this method the hemodynamics of the aorta can be precisely visualized.[3,4] The purpose of this study was to investigate whether this 4D-Flow technique could visualize hemodynamics of a silicon intracranial aneurysm model.

Materials and Methods

Phantom

A Silicon Intracranial Aneurysm Model 3 Times Actual Size. Rotational digital subtraction angiography was performed for a 67-year-old woman with an unruptured right middle cerebral artery bifurcation aneurysm. We obtained a 3D dataset of the right internal carotid angiogram with frame rate of 8.8, matrix of 512 × 512, and with 15 mL of iodinated contrast material (injection rate of 3 mL/s). The greatest dimension of this intracranial aneurysm was 10 mm. The aspect ratio (defined as depth/neck width)[5,6] of the aneurysm was 4.8. This 3D dataset of the right internal carotid angiogram was reconstructed into multiple 2D axial sections with the thickness of 0.5 mm. These DICOM datasets were processed to reconstruct the lumen of the vessels in 3 dimensions and then transferred to a 3D printer by using powders and adhesive to produce a master cast of the vascular lumen. Based on this master cast, a realistic silicon model, 3 times actual size, containing the lumen of the original vessels was then constructed (S. Inagawa, unpublished data). Therefore, the size of the intracranial aneurysm in our model was 30 mm.

Flow Velocity Profile of the Right Middle Cerebral Artery of the Patient. Flow velocity measurement was performed with a 1.5T MR unit (Signa Infinity TwinSpeed with Excite XI [version 11] GE Medical Systems, Milwaukee, Wis) using 2D cine phase contrast MR imaging. The imaging parameters were as follows: repetition time (TR)/echo time (TE)/number of excitation (NEX), 29/5.6/2; field of view (FOV), 100 × 100 mm; matrix, 192 × 128; thickness, 4 mm; velocity encoding (VENC), 80 cm/s; imaging time, 3 minute 5 seconds; imaging plane, sagittal plane; number of phases during one cardiac cycle, 30. Flow velocity profile of the M1 segment of the right middle cerebral artery of this patient was calculated by a workstation. Patient's pulse rate was 84 beats/min, systolic maximum velocity was 44.8 cm/s, and average velocity was 26.2 cm/s. Reynolds number is the ratio of inertial to viscous forces in a fluid. The Reynolds number ranged from 102.1 to 350.5 and was 205.5 on the average velocity in the right middle cerebral artery of the patient. The Womersley parameter represents the ratio of the vascular diameter to the oscillating boundary layer thickness. The Womersley parameter in the middle cerebral artery of this patient was 2.24. The peak systolic and average velocity in this patient were lower than those of previously published data and they were thought to depend on the patient's age.[7,8]

Phantom Circuit. A phantom circuit was a closed circuit with a reservoir tank, a computer controller, a pulsatile pump (CardioFlow 1000MR; Shelly Medical Imaging Technologies Company), the silicon model, and simulation vessel. We ran a 53% weight glycerin solution (T1 value, 1005 ms; T2 value, 86 ms; kinematic viscosity, 14.6×10^{-6} m^2/s, temperature; around 20° centigrade) in pulsatile flow with the cardiac cycle of 2 seconds by using the pump. We measured relaxation times with the MR scanner, viscosity with a viscosimeter, and temperature with a thermometer. Flow velocity measurement was done with the 1.5T MR unit using 2D cine phase contrast MR imaging. The imaging parameters were as follows: TR/

Received September 18, 2005; accepted after revision December 21.

From the Department of Radiology (H.I., H.T., H.S.), Hamamatsu University, School of Medicine, Hamamatsu, Japan; GE Yokogawa Medical Systems, Tokyo, Japan (M.H.); Renaissance of Technology Corporation, Hamamatsu, Japan (T.K.); Department of Radiology (M.T.A., M.M., N.J.P.), Stanford University School of Medicine, Stanford, Calif; and Department of Diagnostic Radiology, Medical Physics (M.M.), University Hospital Freiburg, Freiburg, Germany.

This article was presented previously at the 43rd Annual Meeting of the American Society of Neuroradiology; 2005 May 21–27; Toronto, Canada.

Address correspondence to Haruo Isoda, MD, PhD, Department of Radiology, Hamamatsu University, School of Medicine, 1-20-one Handayama, Hamamatsu, Shizuoka, 431-3192 Japan.

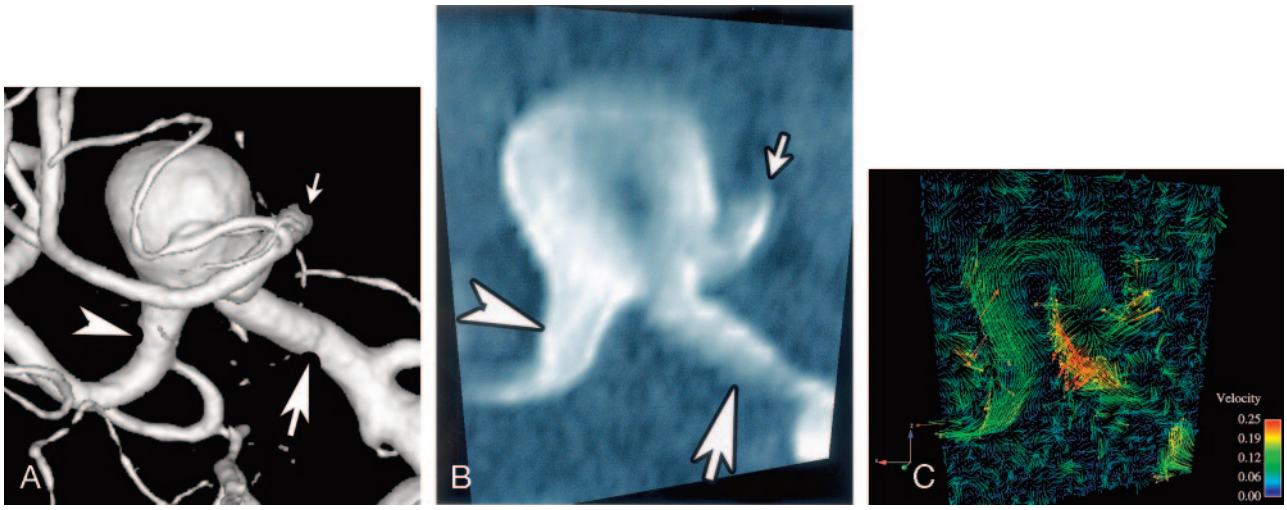

Fig 1. Anteroposterior views of rotational angiogram, magnitude image, and 2D velocity vector field traversing M1 segment and two M2 segments of the right middle cerebral artery (MCA).

A, A surface rendering image obtained from rotational digital subtraction angiogram of the right internal carotid artery reveals that the blood flow moves through the M1 segment of right middle cerebral artery (MCA) (*white arrow*) and then diverges into the two M2 segments (anterior trunk of MCA [*white small arrow*] and posterior trunk of MCA [*white arrowhead*]). There is an aneurysm in this bifurcation of MCA.

B, A magnitude image traversing M1 segment and two M2 segments of the right MCA. *White arrow,* M1 segment; *white small arrow,* anterior trunk of MCA; *white arrowhead,* posterior trunk of MCA.

C, 2D velocity vector field traversing the M1 segment and two M2 segments of right MCA shows counter-clockwise vortex flow in the aneurysm. It demonstrates flow velocities near the vascular wall. 2D velocity vector fields can be displayed as cine images like a movie on a computer display. Numbers and colors correspond with flow rate in the legend at the right side in the figure regarding 2D velocity vector fields. Units in meters per second. Flow rate in the aneurysm is less than 15 cm/s.

TE/NEX, 29/5.2/1; FOV, 160 × 160 mm; matrix, 256 × 128; thickness, 4 mm; VENC, 150 cm/s; imaging time, 4 minutes 18 seconds; number of phases during 1 cardiac cycle, 20. Flow velocity profile of the M1 segment of the middle cerebral artery of this vascular model was calculated by a workstation. The Reynolds number ranged from 80.8 to 584.3 and was 262.5 on the average velocity in the right middle cerebral artery of the silicon model. The Womersley parameter was 2.41. Matching the Reynolds number and the Womersley parameter is the most important consideration in guaranteeing similarity of in vivo and in vitro hemodynamics. To match these nondimensional parameters the velocity and cardiac cycle were adjusted and were therefore different between our model and the patient. The Reynolds number and the Womersley parameter in our model were similar to that in humans so blood flow conditions in the patient were reproduced in our silicon model.

Imaging Method of 4D-Flow

MR Scanner. We used a 1.5T MR scanner (Signa Infinity Twinspeed with Excite XI [version 11]; General Electric) with a commercially available quadrature head coil.

Imaging Sequence. Imaging sequence of 4D-Flow was derived from radio-frequency-spoiled gradient-echo sequence.[3] Imaging was retrospectively gated by electrocardiogram wave produced by the controller of the pulsatile pump. The sequence used a segmented acquisition in the section direction, in which 4 sections were acquired per RR interval and thus, with the 3 encodings and one reference encoding, the true temporal resolution of the data was 4 × 4 × TR. The reconstruction retrospectively created the 20 temporal phases by using linear interpolation. The phase images encoded for x, y, and z directions were corrected by a correction for Maxwell phase effects[9] and the Markl-Bammer correction,[10] and 3D velocity data for each 3D voxel was generated. The data including velocity components in x, y, and z direction and time provided us with 4D-Flow information.

Imaging Parameter. The imaging parameters were as follows: TR/TE/NEX, 5.8/2.1/1; flip angle, 15°; FOV, 140 × 140 × 108 mm; matrix, 160 × 160 × 36; voxel size, 0.88 × 0.88 × 3 mm; VENC, 20 cm/s; imaging time, 48 minutes; imaging plane, transverse plane; maximum gradient magnetic field, 40 mT/m; slew rate, 150 T/m/ms. VENC was set to 20 cm/s, because the intraaneurysmal flow velocity was estimated to be very low based on the large number of the aspect ratio of this aneurysm model.[5,6]

Postprocessing. The data obtained by 4D-Flow were converted into a data format suitable for flow visualization software (EnSight; Computational Engineering International, Apex, NC) by personal computer (Intel Pentium4 CPU, 3.2 GHz, 2 GB of RAM, Linux OS) in approximately 90 minutes. We forwarded these converted data to another personal computer (Intel Pentium4 CPU, 3.2 GHz, 2 GB of RAM, Windows XP) and calculated time-resolved 2D velocity vector fields and time-resolved 3D streamlines with the use of visualization software "EnSight." We processed each set of images within 5 minutes for a total processing time of approximately 1 hour.

We define some of our visualization tools: 2D velocity vector fields are arbitrary 2D planes extracted from the 3D imaging volume; 3-directional velocities are displayed over time as color-coded vector fields;[4] 3D streamlines are integrated traces along instantaneous velocity vector field, color coded according to the local velocity magnitude;[4] the flow rate was shown by a color displayed in each legend.

Results

We obtained 2D velocity vector fields on arbitrary planes (Fig 1), and they were displayed as cine images like a movie on a computer display. 2D velocity vector fields clearly demonstrated flow velocity near the vascular wall. Flow rate in the aneurysm was less than 15 cm/s.

We obtained time-resolved 3D streamlines of the intracranial aneurysm and adjacent arteries (Figs 2 and 3) when we

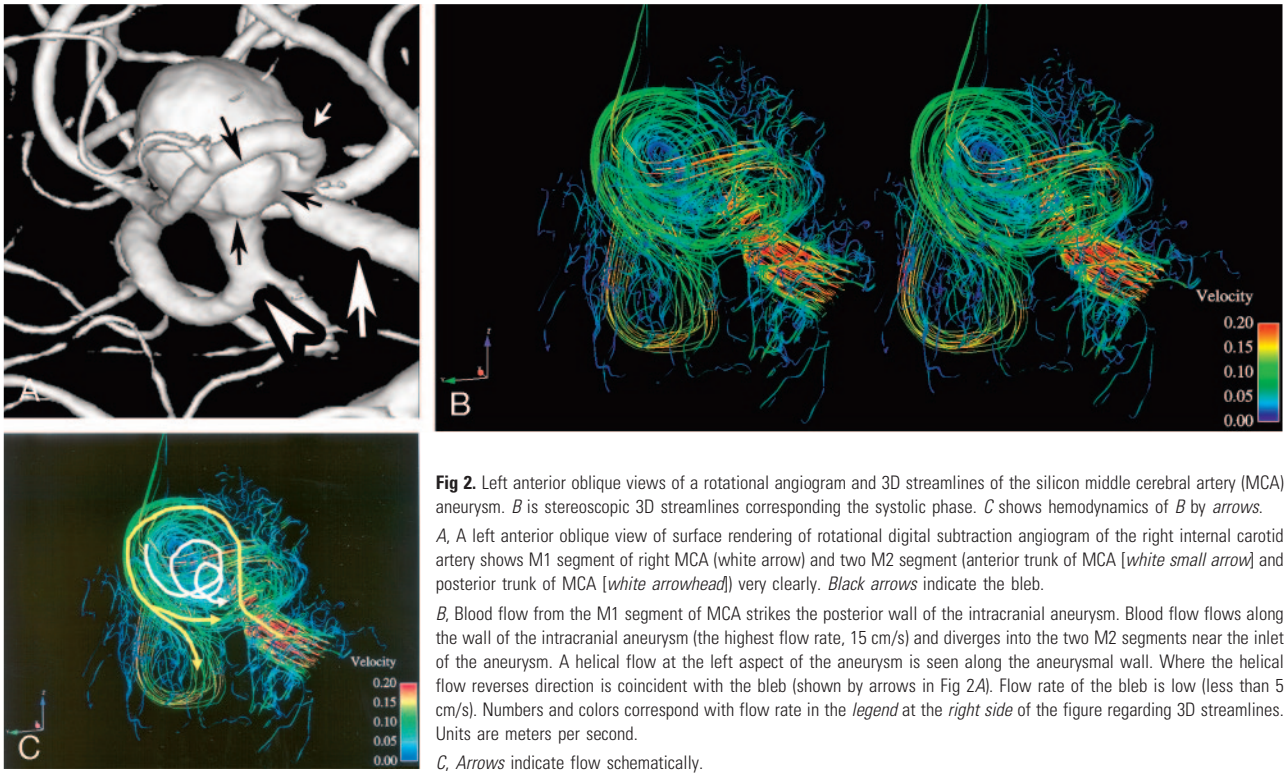

Fig 2. Left anterior oblique views of a rotational angiogram and 3D streamlines of the silicon middle cerebral artery (MCA) aneurysm. *B* is stereoscopic 3D streamlines corresponding the systolic phase. *C* shows hemodynamics of *B* by *arrows*.

A, A left anterior oblique view of surface rendering of rotational digital subtraction angiogram of the right internal carotid artery shows M1 segment of right MCA (white arrow) and two M2 segment (anterior trunk of MCA [*white small arrow*] and posterior trunk of MCA [*white arrowhead*]) very clearly. *Black arrows* indicate the bleb.

B, Blood flow from the M1 segment of MCA strikes the posterior wall of the intracranial aneurysm. Blood flow flows along the wall of the intracranial aneurysm (the highest flow rate, 15 cm/s) and diverges into the two M2 segments near the inlet of the aneurysm. A helical flow at the left aspect of the aneurysm is seen along the aneurysmal wall. Where the helical flow reverses direction is coincident with the bleb (shown by arrows in Fig 2*A*). Flow rate of the bleb is low (less than 5 cm/s). Numbers and colors correspond with flow rate in the *legend* at the *right side* of the figure regarding 3D streamlines. Units are meters per second.

C, *Arrows* indicate flow schematically.

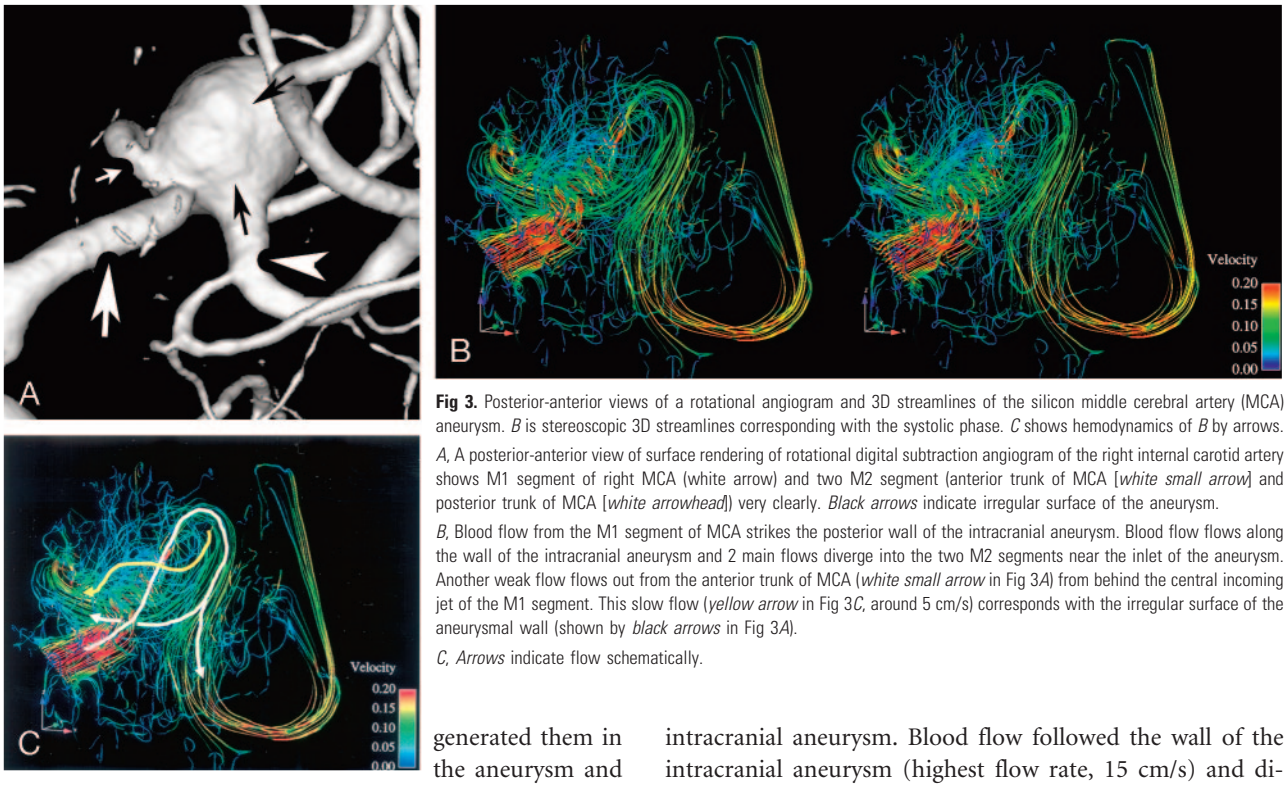

Fig 3. Posterior-anterior views of a rotational angiogram and 3D streamlines of the silicon middle cerebral artery (MCA) aneurysm. *B* is stereoscopic 3D streamlines corresponding with the systolic phase. *C* shows hemodynamics of *B* by arrows.

A, A posterior-anterior view of surface rendering of rotational digital subtraction angiogram of the right internal carotid artery shows M1 segment of right MCA (white arrow) and two M2 segment (anterior trunk of MCA [*white small arrow*] and posterior trunk of MCA [*white arrowhead*]) very clearly. *Black arrows* indicate irregular surface of the aneurysm.

B, Blood flow from the M1 segment of MCA strikes the posterior wall of the intracranial aneurysm. Blood flow flows along the wall of the intracranial aneurysm and 2 main flows diverge into the two M2 segments near the inlet of the aneurysm. Another weak flow flows out from the anterior trunk of MCA (*white small arrow* in Fig 3*A*) from behind the central incoming jet of the M1 segment. This slow flow (*yellow arrow* in Fig 3*C*, around 5 cm/s) corresponds with the irregular surface of the aneurysmal wall (shown by *black arrows* in Fig 3*A*).

C, *Arrows* indicate flow schematically.

generated them in the aneurysm and the M1 segment of the middle cerebral artery. We were able to observe cine images of 3D streamlines from any direction (Figs 2 and 3).

Based on the kinematic display of 3D streamlines rotating along the head-foot axis during systolic phase, hemodynamics of this middle cerebral artery bifurcation aneurysm were the following (Figs 2 and 3): Blood flow from the M1 segment of middle cerebral artery (MCA) struck the posterior wall of the intracranial aneurysm. Blood flow followed the wall of the intracranial aneurysm (highest flow rate, 15 cm/s) and diverged into the 2 M2 segments near the inlet of the aneurysm. A helical flow at the left aspect of the aneurysm was seen along the aneurysmal wall. Where the helical flow reversed direction was coincident with the bleb. Flow rate of the bleb was low (less than 5 cm/s). Helical flow continued to flow into the center of the aneurysm from the bleb. Flow rate was less than 5 cm/s. Two blood flows flow out from the anterior trunk of MCA peripheral to the central incoming jet of the M1 seg-

ment. One of these flows, flowing at the posterior aspect of the aneurysm with slow flow of around 5 cm/s, corresponded with the irregular surface of the aneurysmal wall.

Discussion

Most intracranial aneurysms occur at the bifurcation of the arteries around the circle of Willis, suggesting that hemodynamics is an important factor in the development of intracranial aneurysm and their later progress. Because of the importance of hemodynamics, in vitro blood flow analysis,[1,11,12] in vivo blood flow analysis with animals,[5] and computational fluid dynamics[13,14] of intracranial aneurysms have been performed so far.

Time-resolved 3D dataset of flow velocity information in x, y, and z direction were obtained in this 4D-Flow imaging technique. 2D velocity vector fields and 3D streamlines demonstrated hemodynamics in the intracranial aneurysm model very clearly as shown in the Results section. The bleb was present at the left aspect of this aneurysm model, where the helical flow with lower flow velocity reversed direction. Slow blood flow in the bleb was also observed in articles published previously.[5,14] However, we did not have enough evidence that this kind of local hemodynamics existed before the bleb was formed. Future study is necessary.

Previously obtained 2D cine phase-contrast MR imaging enabled us to measure flow velocity on the individually imaged plane, because it included only 2D spatial blood flow information and time. In this 4D-Flow imaging, 4D blood flow information, including 3D spatial flow information and time dimension, were obtained. Time-resolved images of 3D streamlines viewed from any direction and time-resolved 2D velocity vector fields on arbitrary planes could be obtained. Therefore, we were able to analyze hemodynamics of the MCA bifurcation aneurysm very well with the use of 4D-Flow. Imaging time for 4D-Flow was approximately 48 minutes in this study, data reconstruction for visualization software format was 90 minutes, and hemodynamic analysis with the visualization software was approximately 1 hour. The 4D-Flow hemodynamic analysis was less costly and less time-consuming than other in vitro blood flow analyses, such as particle image velocimetry, laser Doppler velocimetry, or computational fluid dynamics.

One current limitation is the setting of VENC. We must choose the proper VENC to prevent aliasing, because higher blood velocity will alias by producing a higher phase shift. However, higher VENC is not suitable for visualizing slow flow in the aneurysms and the slow flow along the vascular wall. In this study, we chose a VENC of 20 cm/s; therefore, blood velocities aliased in the adjacent M1 segment of the right MCA.

The acquisition time for 4D-Flow is longer than other routine MR imaging however, we think that this technique can be applied for in vivo hemodynamic analysis for human intracranial aneurysms. Spatial resolution of the 4D-Flow is low at present; in the future, however, we will be able to obtain better images with much higher spatial resolution by using 3T MR scanners and better imaging techniques.

Conclusions

In conclusion, 4D-Flow demonstrated time-resolved 2D velocity vector fields and 3D streamlines showing hemodynamics of an intracranial aneurysm and parent arteries in a silicon aneurysm model. We also noticed a lower flow velocity in a bleb located where a helical flow reversed direction.

References

1. Imbesi SG, Kerber CW. **Analysis of slipstream flow in two ruptured intracranial cerebral aneurysms.** *AJNR Am J Neuroradiol* 1999;20:1703–05
2. Tateshima S, Grinstead J, Sinha S, et al. **Intraaneurysmal flow visualization by using phase-contrast magnetic resonance imaging: feasibility study based on a geometrically realistic in vitro aneurysm model.** *J Neurosurg* 2004;100:1041–48
3. Markl M, Chan FP, Alley MT, et al. **Time-resolved three-dimensional phase-contrast MRI.** *J Magn Reson Imaging* 2003;17:499–506
4. Markl M, Draney MT, Hope MD, et al. **Time-resolved 3-dimensional velocity mapping in the thoracic aorta: visualization of 3-directional blood flow patterns in healthy volunteers and patients.** *J Comput Assist Tomogr* 2004;28:459–68
5. Ujiie H, Tachibana H, Hiramatsu O, et al. **Effects of size and shape (aspect ratio) on the hemodynamics of saccular aneurysms: a possible index for surgical treatment of intracranial aneurysms.** *Neurosurgery* 1999;45:119–29
6. Ujiie H, Tamano Y, Sasaki K, et al. **Is the aspect ratio a reliable index for predicting the rupture of a saccular aneurysm?** *Neurosurgery* 2001;48:495–502
7. Valdueza JM, Balzer JO, Villringer A, et al. **Changes in blood flow velocity and diameter of the middle cerebral artery during hyperventilation: assessment with MR and transcranial Doppler sonography.** *AJNR Am J Neuroradiol* 1997;18:1929–34
8. Stock KW, Wetzel SG, Lyrer PA, et al. **Quantification of blood flow in the middle cerebral artery with phase-contrast MR imaging.** *Eur Radiol* 2000;10:1795–800
9. Bernstein MA, Zhou XJ, Polzin JA, et al. **Concomitant gradient terms in phase contrast MR: analysis and correction.** *Magn Reson Med* 1998;39:300–08
10. Markl M, Bammer R, Alley MT, et al. **Generalized reconstruction of phase contrast MRI: analysis and correction of the effect of gradient field distortions.** *Magn Reson Med* 2003;50:791–801
11. Isoda H, Inagawa S, Takeda H, et al. **Preliminary study of tagged MR image velocimetry in a replica of an intracranial aneurysm.** *AJNR Am J Neuroradiol* 2003;24:604–07
12. Tateshima S, Murayama Y, Villablanca JP, et al. **In vitro measurement of fluid-induced wall shear stress in unruptured cerebral aneurysms harboring blebs.** *Stroke* 2003;34:187–92
13. Hassan T, Timofeev EV, Saito T, et al. **Computational replicas: anatomic reconstructions of cerebral vessels as volume numerical grids at three-dimensional angiography.** *AJNR Am J Neuroradiol* 2004;25:1356–65
14. Shojima M, Oshima M, Takagi K, et al. **Magnitude and role of wall shear stress on cerebral aneurysm: computational fluid dynamic study of 20 middle cerebral artery aneurysms.** *Stroke* 2004;35:2500–05